Article

Discovery Medicine 2026; 38(208): 1516–1528
https://doi.org/10.24976/Discov.Med.202638208.118

Comprehensive 16S rRNA Sequencing and Untargeted Metabolomics Analysis Reveal the Mechanism of Oral Microorganisms in Rat Dental Caries

Min Sheng[1,2,*]

[1]Department of Stomatology, Shaoxing Maternity and Child Health Care Hospital, 312000 Shaoxing, Zhejiang, China
[2]Maternity and Child Health Care Affiliated Hospital, Shaoxing University, 312000 Shaoxing, Zhejiang, China
*Correspondence: shengmin@zuaa.zju.edu.cn (Min Sheng)
Submitted: 9 March 2026 Revised: 7 April 2026 Accepted: 22 April 2026 Published: 20 May 2026

Background: This study integrated 16S ribosomal ribonucleic acid sequencing and untargeted metabolomics to investigate the mechanisms by which oral microorganisms and *Lacticaseibacillus rhamnosus* (LGG) influence dental caries development in rats.
Methods: A rat caries model was established to examine the effects of different interventions, including healthy dental plaque suspension (NC_R), caries-associated plaque suspension (M_R), and the probiotic LGG, on oral microbial composition, metabolic profiles, and caries severity.
Results: The caries model group exhibited ecological dysbiosis, characterized by a significant increase in the abundance of cariogenic bacteria such as *Streptococcus mutans* and a decrease in health-associated genera like *Veillonella*. Metabolomic analysis identified 105 significantly differential metabolites between the Model and Normal Control (NC) groups. Kyoto Encyclopedia of Genes and Genomes pathway enrichment classification revealed that carbohydrate metabolism pathways were significantly enriched in the Model group, whereas lipid metabolism and cofactor metabolism pathways exhibited higher activity in the NC group. Notably, the sphingolipid metabolism pathway showed the highest significance in differential metabolite enrichment. Probiotic intervention, particularly the combined application of LGG and NC_R, substantially reversed the levels of abnormal metabolites, improved enamel surface area, volume, and mineral density ($p < 0.05$), and reduced caries scores ($p < 0.05$).
Conclusion: By integrating microbiome and metabolomics analyses, this study elucidates the interplay between microbial dysbiosis and metabolic dysregulation in the pathogenesis of dental caries. It further reveals a novel anti-caries mechanism of probiotics through their modulation of oral microecological balance and host metabolic networks, particularly via key pathways such as sphingolipid metabolism. This provides experimental evidence for the development of precise caries prevention and control strategies based on microecological regulation.

Keywords: oral microorganisms; caries; probiotics; 16S ribosomal ribonucleic acid sequencing; metabolomics analysis

Introduction

Dental caries is the most common chronic disease in both childhood and adulthood, with early childhood caries (ECC) being particularly prominent, affecting approximately 530 million children worldwide [1]. There are significant geographical variations in its prevalence, with a combined prevalence of about 49% across 49 countries, the lowest being in Japan (20.6%) and Greece (19.3%) [2]. However, the situation in China is concerning. Data from Guangdong Province from 2015 to 2016 show that the prevalence of ECC in children aged 3–5 years is as high as 68.3%, while the filling rate is only 1.2% [3]. National surveys indicate that the prevalence of dental caries in children increased from 27.05% in 2005 to 37.92% in 2015 [4], and the overall caries prevalence among schoolchildren aged 6–8 in Hangzhou is approximately 52.78% [5]. These findings highlight the severe challenges in children's oral health and underscore the urgent need for enhanced prevention and treatment efforts.

The pathogenesis of dental caries is complex, involving genetic, behavioral, environmental, and microbial factors. Modern research suggests that cariogenic microorganisms colonize dental plaque biofilms early in life and initiate disease under favorable conditions. As early as 1984, a study found that the proportion of *Streptococcus mutans* in plaque increased significantly 6 to 24 months before caries diagnosis [6]. With advancements in microbial detection technologies, research has further revealed that caries is not only associated with Streptococcus mutans but also closely related to changes in the abundance of microorganisms such as *Streptococcus sobrinus*, *Actinomyces B19SC*, and *Lactobacillus* [7,8]. Recent comparisons of oral microbiota between caries-active and caries-free children have shown significant differences in dominant microbial communities [9]. Furthermore, integrated analysis of microbial composi-

tion and metabolic characteristics indicates that plaque from severe caries groups exhibits enhanced acid tolerance, with significantly higher abundances of *Streptococcus* and *Prevotella*, suggesting that microbial metabolic function plays a critical role in caries progression [10]. These advances have shifted the understanding of caries mechanisms from a single-pathogen theory to a holistic perspective of oral microecological imbalance.

Streptococcus mutans, as one of the primary cariogenic bacteria, has been widely confirmed for its cariogenic potential [11]. It promotes dense biofilm formation by secreting virulence factors such as extracellular polysaccharides and glucan-binding proteins, and continuously produces acids during metabolism, creating a localized acidic microenvironment that ultimately leads to enamel demineralization [12]. Current strategies for caries prevention and control mainly include physical cleaning, chemical antibacterial agents, and biological regulation. Among these, probiotic interventions have garnered significant attention due to their potential to modulate microbial balance, inhibit pathogenic bacteria, and enhance oral defense. Clinical studies have shown that probiotic-containing mouthwashes significantly inhibit the proliferation of Streptococcus mutans in both children and elderly populations, with effects superior to chlorhexidine [13]. Animal experiments further demonstrate that probiotics such as *Lactobacillus rhamnosus* (LGG), *Limosilactobacillus fermentum*, and *Lactiplantibacillus plantarum*, as well as their combinations, effectively reduce Streptococcus mutans counts in rat oral cavities and mitigate enamel caries severity [14–18].

Current research indicates that the anti-caries mechanisms of probiotics involve multiple pathways, including the secretion of metabolically active products, inhibition of cariogenic bacterial biofilms, competitive adhesion and colonization, and immune regulation [12,19]. However, the specific mechanisms by which healthy oral microbiota maintain microecological homeostasis and resist caries through metabolic regulation, particularly from a metabolomics perspective, remain insufficiently explored. Therefore, this study aims to establish a rat caries model and integrate 16S ribosomal ribonucleic acid (16S rRNA) sequencing with untargeted metabolomics to clarify the critical role of dental plaque microbiota in caries development. It will also preliminarily elucidate the metabolic regulatory mechanisms underlying cariogenesis, identify potential differential metabolites associated with caries progression and probiotic intervention, and screen functional metabolites with anti-caries potential based on metabolic pathway analysis. This research provides experimental evidence for deepening the understanding of microbe-metabolite interactions in caries and for developing metabolically regulated microecological strategies for caries prevention.

Materials and Methods

Experimental Animals

21-day-old male Sprague-Dawley rats (specific pathogen-free grade) were obtained from Shanghai SLAC Laboratory Animal Co., Ltd. (License No. SCXK (Hu) 2022-0004). All rats were maintained in a specific pathogen-free barrier system at Hangzhou Hunter Quality Inspection Biotechnology Co., Ltd. (Facility License No. SYXK (Zhe) 2024-0003) under controlled conditions of 22 $\pm$ 2 °C, 50%–60% relative humidity, a 12 h light/12 h dark cycle, and 15–20 air changes per hour, with food and water available ad libitum. The animal experimental protocol in this study was reviewed and approved by the laboratory animal management and ethics committee of Hangzhou Hunter Testing Biotechnology Co., Ltd. (IACUC/HTYJ-11746-93).

Model Preparation Process

To establish the caries model, rats first received drinking water supplemented with Ampicillin (A800200, Shanghai Macklin Biochemical Co., Ltd., Shanghai, China), chloramphenicol (S17022-25g, Shanghai Yuanye Bio-Technology Co., Ltd., Shanghai, China), and carbenicillin sodium (S17021-10g, Shanghai Yuanye Bio-Technology Co., Ltd., Shanghai, China) (1 g/kg each) for 3 consecutive days to suppress the native oral microbiota [16]. Subsequently, a sterile cotton swab soaked in a cariogenic bacterial suspension (1×10^8 CFU/mL [20]; PBS (phosphate-buffered saline, GNM20012-5, Zhejiang Genosail Biotech Co., Ltd., Jiaxing, China) for the control group) was uniformly applied to the occlusal surfaces of the maxillary and mandibular molars for 15 s, followed by 30 min of fasting without water. This procedure was performed once daily for 5 days. During modeling, tooth surface samples were collected daily with a cotton swab, placed in 1 mL of physiological saline, serially diluted, and plated for bacterial enumeration. Modeling was considered successful when the cariogenic bacterial count exceeded 10^2 CFU/mL; otherwise, the procedure was repeated. At the same time, rats were fed a cariogenic diet and provided with distilled water containing 5% (w/v) sucrose ad libitum for 5 weeks to promote caries progression [16].

Preparation and Grouping of Rat Dental Plaque Suspensions

Oral plaque samples were collected from three healthy rats in the Normal Control (NC) group and three caries rats in the Model group, respectively. The samples were resuspended in sterile PBS containing 1.2% (w/v) carboxymethyl cellulose (V32431, Shanghai yuanye Bio-Technology Co., Ltd., Shanghai, China) to prepare bacterial suspensions at a concentration of 1×10^8 CFU/mL. The pooled suspension from healthy rats was designated as NC_R, while that from caries rats was designated as

M_R. Prior to experimental use, equal volumes of suspension from the three rats within each group were thoroughly mixed [21].

Experimental Grouping

Rats were randomly allocated into seven groups (n = 6 per group): NC, Model, Model+NC_R, Model+M_R, Model+LGG (HZB123071, HuiZao Biotechnology, Microbial Conservation Platform), Model+LGG+NC_R, and Model+LGG+M_R. All animals were fed a cariogenic diet and provided with 5% sucrose water for 5 weeks. The oral interventions were as follows: the NC group received sterile PBS (200 µL/rat/day); the Model group received *Streptococcus mutans* suspension (1×10^8 CFU/mL, 200 µL/rat/day); the Model+NC_R group received co-application of equal volumes (100 µL each) of *Streptococcus mutans* suspension and oral plaque suspension from healthy rats (NC_R); the Model+M_R group received co-application of equal volumes (100 µL each) of *Streptococcus mutans* suspension and oral plaque suspension from caries rats (M_R); the Model+LGG group received co-application of equal volumes (100 µL each) of *Streptococcus mutans* suspension (HZB357747, Wuhan Huizao Biotechnology Co., Ltd., Wuhan, China) and LGG suspension (HZB123071, Wuhan Huizao Biotechnology Co., Ltd., Wuhan, China); the Model+LGG+NC_R group received co-application of *Streptococcus mutans* suspension (100 µL), LGG suspension (50 µL), and NC_R suspension (50 µL); and the Model+LGG+M_R group received co-application of *Streptococcus mutans* suspension (100 µL), LGG suspension (50 µL), and M_R suspension (50 µL). All treatments were administered once daily for 5 consecutive days.

Micro-Computed Tomography (Micro-CT) Analysis

After euthanasia by an overdose of CO_2, mandibular molar samples were collected from rats. The samples were rinsed with PBS to remove blood residues, fixed in 4% paraformaldehyde for 48 h, followed by PBS rinsing and storage in 75% ethanol. The complete mandibular molar region was scanned using Micro-CT (SkyScan1276, Bruker, Kontich, Belgium) (scanning parameters: 70 kV voltage, 200 µA current, Al 0.5 mm filter, 10 µm resolution, medium resolution mode) and three-dimensional reconstruction was performed. Enamel was segmented from the molar structure by applying a fixed threshold, and its surface area and volume were calculated. Mineral density of enamel was quantitatively determined based on calibration with hydroxyapatite phantoms of known densities.

Caries Scoring of Rat

The mandibles were aseptically dissected, cleaned of soft tissue, washed, and dried, followed by fixation in 4% paraformaldehyde for 24 h. The samples were then stained in 0.4% murexide (S19162, Shanghai yuanye Bio-Technology Co., Ltd., Shanghai, China) for 18 h, rinsed with distilled water to remove excess dye, and air-dried at room temperature. The right mandible was sectioned mesiodistally along the dental arch using a slicing disc. The staining penetration was observed under a stereomicroscope (SZM7045, Ningbo Sunny Instruments Co., Ltd., Ningbo, China) and photographed. Caries severity in the right mandibular molars was quantitatively scored according to the Keyes scoring system [18]. Occlusal pit and fissure caries are classified into four grades: enamel caries (E), where the lesion is confined to the enamel layer; slight dentinal caries (Ds), involving the enamel and extending into the outer quarter of dentin; moderate dentinal caries (Dm), extending to between one-quarter and three-quarters of dentin thickness; and extensive dentinal caries (Dx), exceeding three-quarters of dentin thickness or involving the full thickness of dentin. The scoring units for pit and fissure caries in each mandibular molar were 7 for the first molar, 5 for the second molar, and 2 for the third molar. According to the Keyes scoring method [22], the extent of carious lesions in rat molars is assessed visually, with scores assigned to the four grades of caries and summed to evaluate the overall severity of molar caries.

Analysis of Changes in the Microbial Spectrum of Rat Dental Caries by 16S rRNA Sequencing

In this study, 16S rRNA gene sequencing was employed to systematically analyze changes in the microbial composition of rat dental plaque. On the final day of the experiment, supragingival plaque samples were collected from all accessible tooth surfaces using sterile Gracey curettes and immediately stored at –80 °C. Deoxyribonucleic acid was extracted from samples, and after quality control, the V3-V4 hypervariable region of the bacterial 16S rRNA gene was amplified by polymerase chain reaction using universal primers 338F (ACTCCTACGGGAGGCAGCAG) and 806R (GGACTACHVGGGTWTCTAAT). The amplified products were purified and used to construct sequencing libraries, followed by paired-end sequencing on an Illumina MiSeq/Novaseq platform (Illumina, San Diego, CA, USA). Raw sequencing data were processed by adapter removal and low-quality filtering, assembled, and subjected to chimera removal to obtain high-quality effective sequences. Operational Taxonomic Units (OTUs) or Amplicon Sequence Variants were generated through clustering or denoising analysis, and taxonomic annotation was performed using the SILVA or Greengenes database. Finally, based on the annotation results, comprehensive bioinformatics analyses, including alpha and beta diversity analysis, species composition profiling, and intergroup differential analysis, were conducted using the QIIME2 platform and relevant R packages.

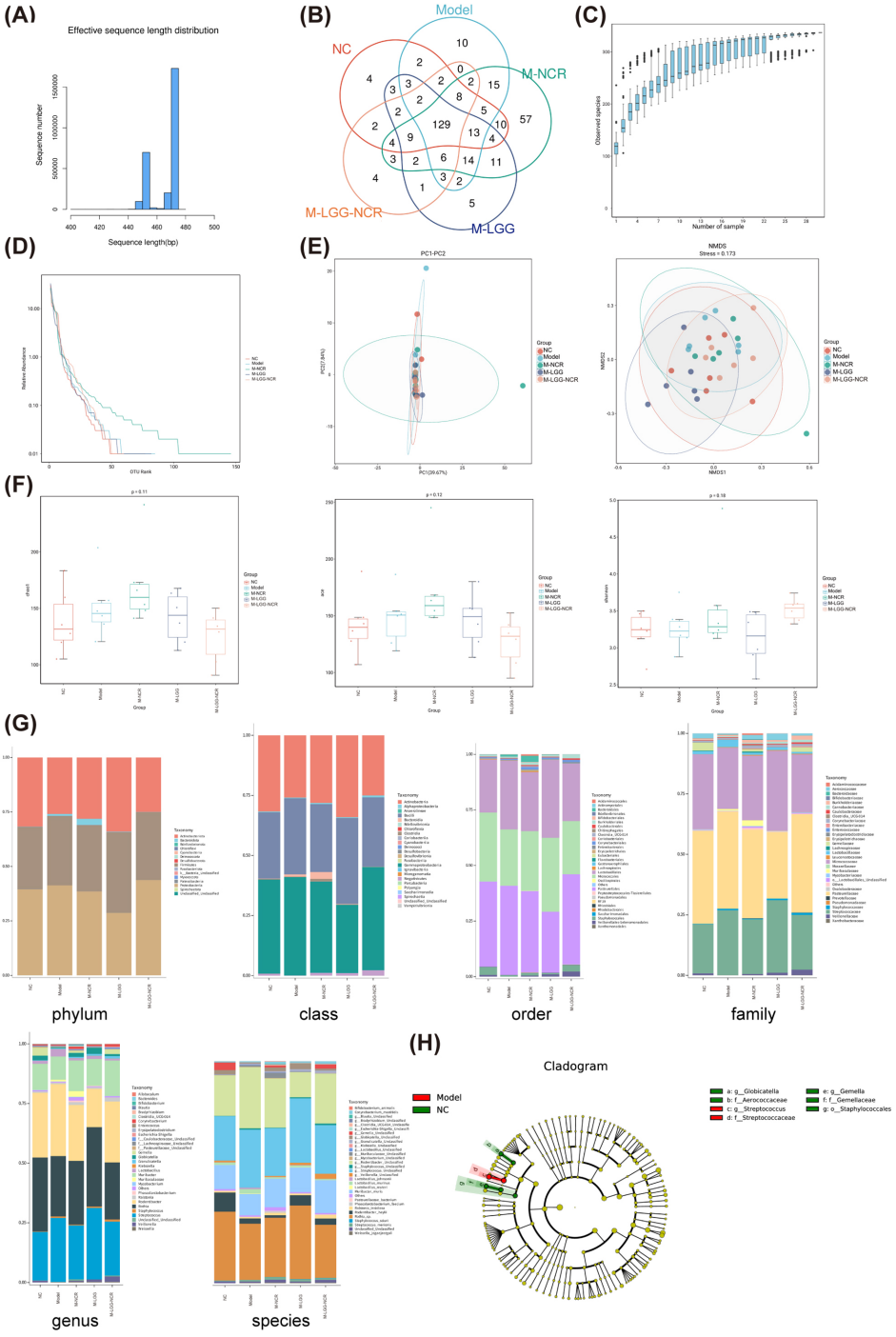

Fig. 1. Analysis of the dental plaque microbiome in rats from each group based on 16S ribosomal ribonucleic acid sequencing. (A) Overview of sequencing data: Distribution of effective sequence lengths per sample. (B) Core and unique Operational Taxonomic Unit analysis: Operational Taxonomic Units shared and unique among the five groups. (C) Species accumulation curve: Evaluating whether sequencing depth is sufficient to reflect sample species diversity. (D) Rank-abundance curves: Assessing the evenness of species distribution within each sample. (E) β diversity analysis: Principal Coordinates Analysis and Non-metric Multidimensional Scaling based on Bray-Curtis distance, illustrating differences in microbial community structure between groups. (F) α diversity analysis: Comparison of Chao1 index, ace index, and Shannon index among groups. (G) Microbial community composition: Relative species abundance at the phylum, class, order, family, genus, and species levels for each group. (H) Cladogram, identification of biomarker taxa (linear discriminant analysis effect size analysis): Microbial taxa showing significant differences between the NC group and Model groups. **Note**: NC, Normal Control group; Model, Model group; M-NCR, Model+NC_R group; M-LGG, Model+LGG group; M-LGG-NCR, Model+LGG+NC_R group.

Untargeted Metabolomics Analysis of Metabolomic Changes in Rat Dental Caries

This study employed an untargeted metabolomics approach to analyze the metabolic profiles of dental plaque and saliva in rats, aiming to elucidate the alterations in metabolic signaling pathways underlying the anti-caries effects of healthy microbiota and probiotic interventions. The goal was to identify key differential metabolites and provide a metabolic-level rationale for optimizing probiotic-based anti-caries formulations. On the final day of the experiment, supragingival plaque samples were gently collected from all accessible exposed tooth surfaces using sterile Gracey curettes, while saliva samples (via throat swabs) were concurrently obtained. Samples from each rat were stored individually, immediately flash-frozen in liquid nitrogen, and preserved at –80 °C until analysis. For sample pre-processing, tissues were thawed on ice, accurately weighed, and metabolites were extracted by adding ice-cold methanol-water solution. Following vortex mixing and ultrasonication, the mixture was subjected to high-speed centrifugation at 4 °C (12,000 ×g, 15 min). The supernatant was collected and filtered through a 0.22 µm microporous membrane to obtain the test solution. Chromatographic separation of target compounds was performed using a Vanquish ultra-high-performance liquid chromatography system (Thermo Fisher Scientific, Waltham, MA, USA) equipped with a Waters ACQUITY ultra-high-performance liquid chromatography ethylene bridged hybrid Amide column (2.1 mm × 50 mm, 1.7 µm). An Orbitrap Exploris 120 mass spectrometer, controlled by Xcalibur software (version 4.4, Thermo Fisher Scientific, Waltham, MA, USA), was used to acquire both primary and secondary mass spectrometry data. Raw data were converted to mzXML format using ProteoWizard software (v3.0.24054, ProteoWizard, Palo Alto, CA, USA). Metabolite identification was performed using a collaboratively developed R package (version 3.3.3), referencing an in-house database. Subsequently, a custom-developed R package was utilized for visualization analysis. Pathway enrichment and functional annotation were conducted with the Kyoto Encyclopedia of Genes and Genomes (KEGG) database to systematically reveal the metabolic reprogramming features and potential biomarkers associated with the anti-caries effects.

Statistical Analysis

Data are presented as mean ± standard deviation. Statistical analyses were performed using Statistical Package for the Social Sciences 26.0 (IBM Corp., Armonk, NY, USA) and GraphPad Prism 9.0 (GraphPad Software, San Diego, CA, USA). Normality of continuous data was assessed using the Shapiro-Wilk test, and homogeneity of variances was evaluated using Levene's test. For data meeting the assumptions of normality and homogeneity of variance, one-way analysis of variance was used for multiple-group comparisons, followed by Tukey's honest significant difference post hoc test for pairwise comparisons. For data that did not meet these assumptions, the Kruskal-Wallis test was applied for multiple-group comparisons, followed by Dunn's post hoc test with Bonferroni correction for pairwise comparisons. For comparisons between two groups, the independent samples *t*-test or Mann-Whitney U test was used as appropriate. $p < 0.05$ was considered statistically significant.

Results

Analysis of the Dental Plaque Microbiome in Rats From Each Group Based on 16S rRNA Sequencing

Extensive studies indicate that microbiota is involved in caries development. To further explore the underlying mechanisms, this study analyzed the microbiome composition using 16S rRNA gene sequencing. After quality control, approximately 2.2–2.6 million high-quality sequences were obtained from 30 dental plaque samples across five groups (Fig. 1A). Based on a 97% similarity threshold, at the level of OTU taxonomy, 337 OTU were detected, including 129 in five groups (Fig. 1B). The species accumulation curve indicated that species richness plateaued when the sample size reached 28, suggesting sufficient sequencing depth (Fig. 1C). The rank-abundance curve of the M-NCR group was slightly higher than those of other groups, but the difference was not statistically significant (Fig. 1D).

Based on OTU-level data, alpha and beta diversity indices were further calculated to evaluate the richness, diversity, and inter-group differences of the microbial communities. Beta diversity was analyzed using Principal Coordinates Analysis and Non-metric Multidimensional Scaling based on Bray-Curtis distance. The results showed partial overlap among sample points from different groups, with no clear separation between the NC and Model groups (Fig. 1E), suggesting that the overall microbial community structure was not dramatically altered at the beta diversity level (Fig. 1E). In terms of alpha diversity, although the Chao1, ace, and Shannon indices of the M-NCR group were higher than those of other groups, suggesting a trend towards increased microbial richness and diversity in this group, none of these differences reached statistical significance (Fig. 1F).

Differences in microbial community structure across various taxonomic levels were further analyzed (Fig. 1G). Specifically, at the phylum level, the relative abundance of *Bacteroidota* was highest in the M-NCR group; the Model group showed the lowest abundance of *Actinobacteriota*, while the M-LGG group had the lowest abundance of *Proteobacteria*. At the class level, the abundances of *Actinobacteria* and *Negativicutes* were lowest in the Model group, whereas *Bacteroidia* and *Clostridia* were most abundant in the M-NCR group. At the order level, *Staphylococcus* and *Veillonellales-Selenomonadales* were least abundant in the Model group, but showed a

Table 1. Statistical table of up-regulated and down-regulated metabolites in each group.

Group	Model *vs.* M-LGG-NCR	M-NCR *vs.* M-LGG-NCR	NC *vs.* Model	Model *vs.* M-LGG	Model *vs.* M-NCR	M-LGG *vs.* M-LGG-NCR
Total amount	2037	2037	2037	2037	2037	2037
Number of differential metabolites	289	203	105	35	29	101
Number of significantly upregulated metabolites	172	108	43	13	21	83
Number of significantly downregulated metabolites	117	95	62	22	8	18

Note: NC, Normal Control group; Model, Model group; M-NCR, Model+NC_R group; M-LGG, Model+LGG group; M-LGG-NCR, Model+LGG+NC_R group.

gradual increase in the M-NCR, M-LGG, and M-LGG-NCR groups. At the family level, the Model group exhibited the highest abundance of *Lactobacillaceae*, while the abundances of *Aerococcaceae*, *Gemellaceae*, and *Veillonellaceae* were the lowest. At the genus level, the Model group had the highest abundance of *Lactobacillus*, but the lowest abundances of *Globicatella* and *Veillonella*; the M-LGG group showed the highest abundances of *Globicatella* and Rothia; and the M-LGG-NCR group had the highest abundance of *Veillonella*. At the species level, the abundances of *Gemella_Unclassified*, *Rodentibacter_heylii* were markedly lower in the Model group compared to other groups, whereas the abundances of *Lactobacillus_murinus* were significantly higher. Furthermore, in the Model group, the unclassified genus and *Muribacter muris* were more abundant, while *Rodentibacter heylii* were relatively less abundant compared to other groups. Finally, to identify specific microbial taxa within each group, linear discriminant analysis effect size analysis was performed and corresponding cladograms were generated. The results revealed that multiple microbial taxa served as biomarkers between the groups. Specifically, *g_Globicatella*, *f_Aerococcaceae*, *g_Gemella*, *f_Gemellaceae*, and *o_Staphylococcales* were enriched in the NC group, whereas *g_Streptococcus* and *f_Streptococcaceae* were enriched in the Model group (Fig. 1H).

Untargeted Metabolomic Analysis of Dental Plaque and Saliva Samples From Rats in Each Group

Untargeted metabolomic analysis was performed on dental plaque and saliva (throat swab) samples from rats. A total of 30 samples across 5 groups were included in the study. After data preprocessing, 42,171 metabolic features were retained. Among these, 2037 substances were identified by comparison with secondary mass spectrometry libraries (Fig. 2A). As shown in Table 1, the comparative analysis between groups revealed the number of differential metabolites, the number of significantly upregulated metabolites, and the number of significantly downregulated metabolites. The principal component analysis score plot showed that all samples (including quality control samples) were within the 95% confidence interval (Hotelling's T^2 ellipse), indicating the overall distribution trend of the samples and good quality control (Fig. 2B). Hierarchical clustering heatmap results revealed distinct differences in metabolite expression profiles among different groups (Fig. 2C). The patterns of relative abundance changes of metabolites also varied across different groups (Fig. 2D). Analysis of the number of differentially expressed metabolites between groups showed that the comparison between the Model and M-LGG-NCR groups contained the highest total number of metabolites (approximately 300) (Fig. 2E).

Bioinformatics Analysis of Differential Metabolites Between the NC and Model Groups

To further investigate the metabolic alterations associated with caries development, we performed a series of bioinformatics analyses focusing on the significantly differential metabolites between the NC and Model groups. First, the orthogonal partial least squares discriminant analysis score scatter plot indicated that greater horizontal distance between samples reflected larger intergroup differences between NC and Model groups, while closer vertical proximity suggested better intra-group reproducibility (Fig. 3A). Second, based on the volcano plot and hierarchical clustering heatmap, the top 10 significantly upregulated and downregulated differential metabolites between the NC and Model groups were identified. Comparison between the NC and Model groups showed that metabolites including Isovaleramide, PC(P-16:0_18:2(9Z,12Z)), 6-(ethylsulfonyl)-2H-1,4-benzoxazin-3(4H)-one, Eglumetad, N-Methylpropanamide, and n-amylamine were significantly elevated in the Model group (Fig. 4A), while metabolites such as (1s,2s,3r,4r)-4-Aminocyclopentane-1,2,3-Triol, 3-Pyridinecarbonitrile,1,2-dihydro-4-methoxy-2-oxo-, 7,8-Dihydrobiopterin, 4-[(Z)-15,16-dihydroxydotriacont-19-enyl]-2-methyl-2H-uran-5-one, 2-amino-8-hydroxyoctanoate, and 6-(ethylsulfonyl)-2H-1,4-benzoxazin-3(4H)-one were significantly reduced (Fig. 3B).

Subsequently, KEGG pathway enrichment analysis was performed on the differential metabolites. The results revealed that the metabolite levels showed significant differences between the NC and Model groups across multiple KEGG pathways (Fig. 3C). Specifically, metabolites in the NC group were significantly enriched in pathways such as "Global and overview maps", "Lipid metabolism",

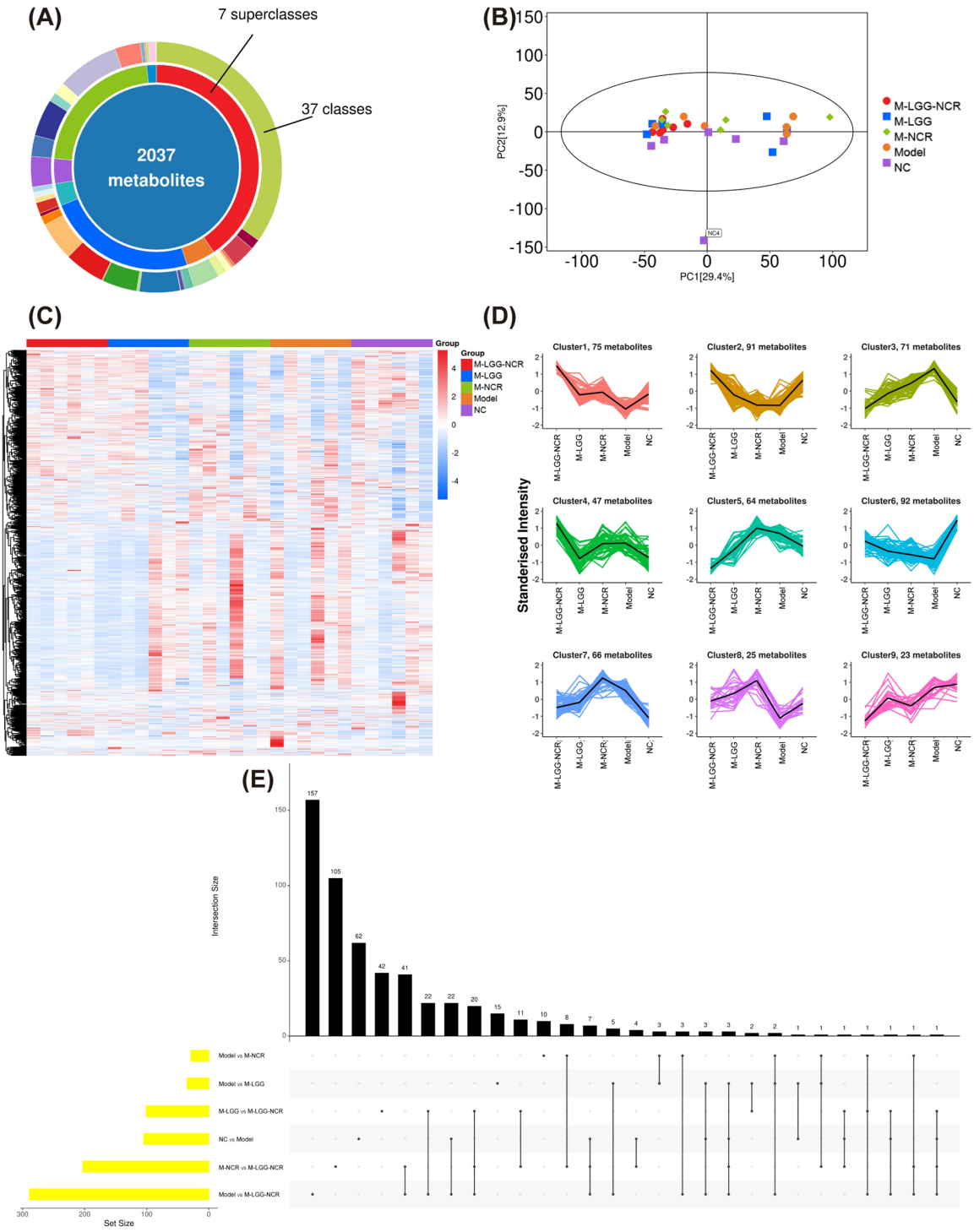

Fig. 2. Untargeted metabolomic analysis of dental plaque and saliva samples from rats in each group. (A) Overview of metabolite feature identification: A total of 42,171 features were retained after preprocessing, of which 2037 were qualitatively identified by matching to secondary mass spectrometry libraries. (B) Principal Component Analysis score plot: All samples are located within the 95% confidence interval, indicating good intra-group reproducibility and an overall grouping trend. (C) Hierarchical clustering heatmap: It shows distinct differences in metabolite expression profiles among different groups. (D) K-Means cluster analysis of differential metabolites in each group. (E) Venn diagram analysis of differential metabolites. Each dot in the figure represents a comparison group, and the Set Size corresponding to each dot represents the number of metabolites contained in the comparison group. The dot connection corresponding to the abscissa of the bar chart represents the comparison of each group, and the ordinate represents the number of different metabolites shared by each group. **Note**: NC, Normal Control group; Model, Model group; M-NCR, Model+NC_R group; M-LGG, Model+LGG group; M-LGG-NCR, Model+LGG+NC_R group.

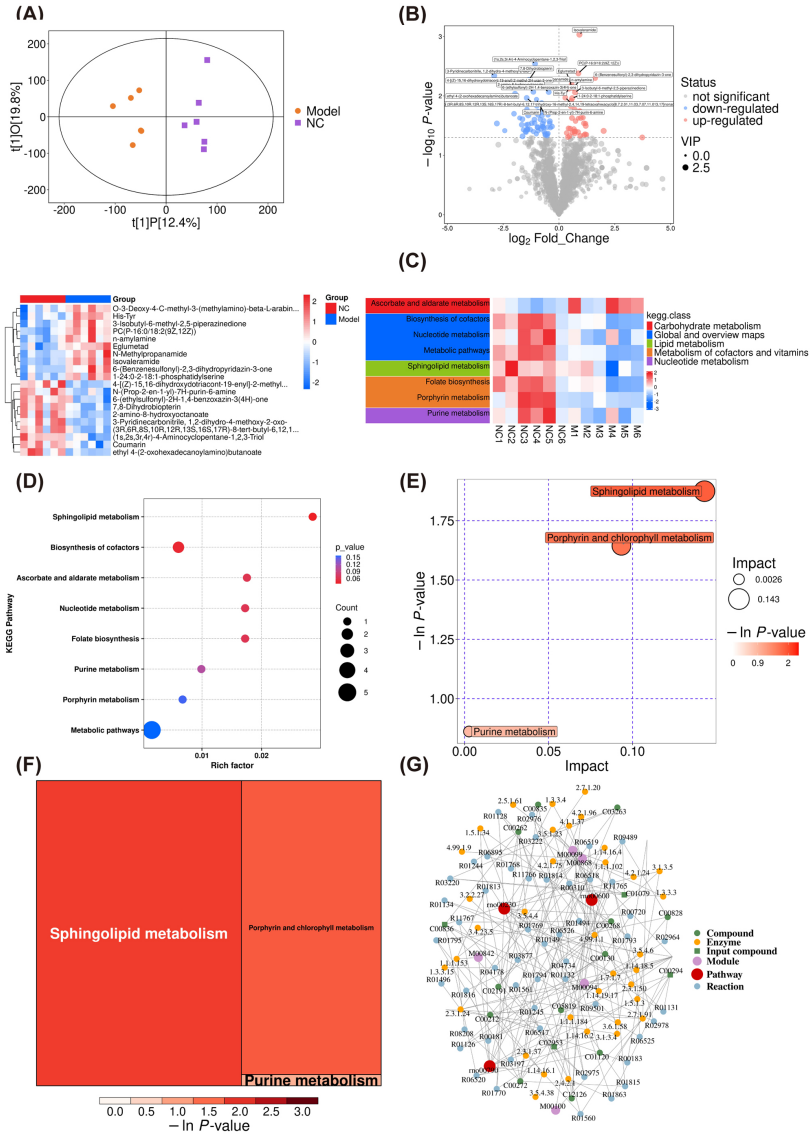

Fig. 3. Bioinformatics analysis of differential metabolites between the NC and Model groups. (A) Orthogonal partial least squares-discriminant analysis score scatter plot. The horizontal distance between samples reflects intergroup differences (NC *vs*. Model), while vertical proximity indicates intra-group reproducibility. (B) Volcano plot displaying metabolites with significant changes (up- and down-regulated). Hierarchical clustering heatmap of the top 10 upregulated and downregulated metabolites between NC and Model groups. (C) Kyoto Encyclopedia of Genes and Genomes (KEGG) heat map of NC group to Model groups. In the figure, the abscissa represents different samples, the ordinate represents KEGG metabolic pathway, and the background color represents different pathway classifications. The color block on the thermogram represents the relative expression of all the differential metabolites annotated in the corresponding position pathway, and the closer the color is to deep red, the higher the sum of the contents of all the different metabolites annotated in the representative pathway. The closer the color is to dark blue, the lower the sum of all the different metabolites. (D) KEGG pathway enrichment analysis (overview): Bar charts showing pathways with the highest number of enriched differential metabolites (top) and pathways with the highest enrichment significance (bottom). (E) KEGG pathway enrichment bubble plots: Visualization of enrichment analysis results. Bubble color intensity represents enrichment significance ($-\log_{10}(p\text{-value})$), and bubble size represents the number of differential metabolites. (F) KEGG pathway enrichment rectangular tree diagram, each square in the rectangular tree diagram represents a metabolic pathway, and the size of the square indicates the size of the influence factor of the pathway in topology analysis. The larger the size, the greater the influence factor. The color of the square represents the *p* value of enrichment analysis (negative natural logarithm, that is, $-\ln(p)$). The deeper the color, the smaller the *p* value, and the more significant the enrichment degree highlighting key pathways such as "Sphingolipid metabolism". (G) Metabolic pathway regulatory interaction network: Constructed based on the KEGG database, illustrating the interactions among key metabolic pathways, associated regulatory enzymes, and differential metabolites. **Note**: NC, Normal Control group; Model, Model group.

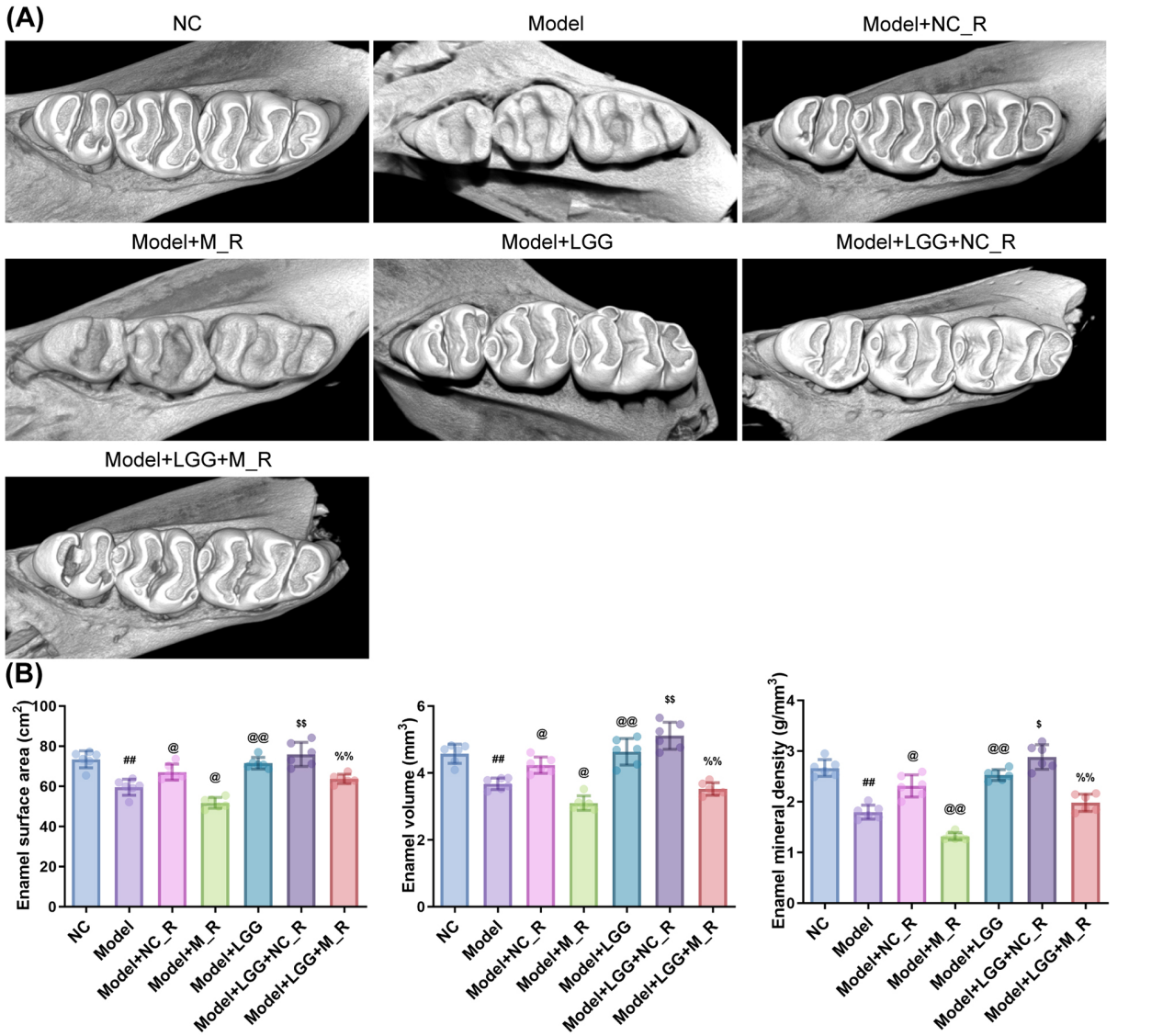

Fig. 4. Effects of different treatments on enamel caries in rat molars as evaluated by Micro-computed Tomography (Micro-CT). (A) Micro-CT scan of mandibular molars of rats in each group. (B) Quantitative results of enamel surface area, enamel volume and enamel mineral density of rats in each group ($n = 6$). Data are presented as mean ± SD. $^{\#\#}p < 0.01$ *vs.* NC group; $^{@}p < 0.05$, $^{@@}p < 0.01$ *vs.* Model group; $^{\$}p < 0.05$, $^{\$\$}p < 0.01$ *vs.* Model+NC_R group; $^{\%\%}p < 0.01$ *vs.* Model+M_R group.

"Metabolism of cofactors and vitamins", and "Nucleotide metabolism". In contrast, metabolites in the Model group were significantly enriched in "Carbohydrate metabolism". In terms of the number of differential metabolites, the overarching "Metabolic pathways" category contained the most hits. Regarding enrichment significance, the "Biosynthesis of cofactors" pathway showed the highest enrichment level (Fig. 3D). The pathway enrichment bubble plot further highlighted that the "Sphingolipid metabolism" pathway had the darkest color (indicating the smallest *p*-value) and was the most significantly enriched, suggesting that the differential metabolites might have the greatest impact on this pathway and warranting focused investigation in follow-up studies (Fig. 3E,F). Finally, pathway search and regulatory interaction network analysis based on the KEGG database visually delineated the complex interactions among metabolic pathways, associated regulatory enzymes, and the differential metabolites (Fig. 3G). See **Supplementary Figs. 1–5** for the metabolic analysis of other groups.

Effects of Different Treatments on Enamel Caries in Rat Molars as Evaluated by Micro-CT

The extent of caries in rat mandibular molars was assessed using Micro-CT. Compared with the NC group, the Model group exhibited significant reductions in enamel surface area, enamel volume, and enamel mineral density (Fig. 4A,B) ($p < 0.01$). Compared with the Model

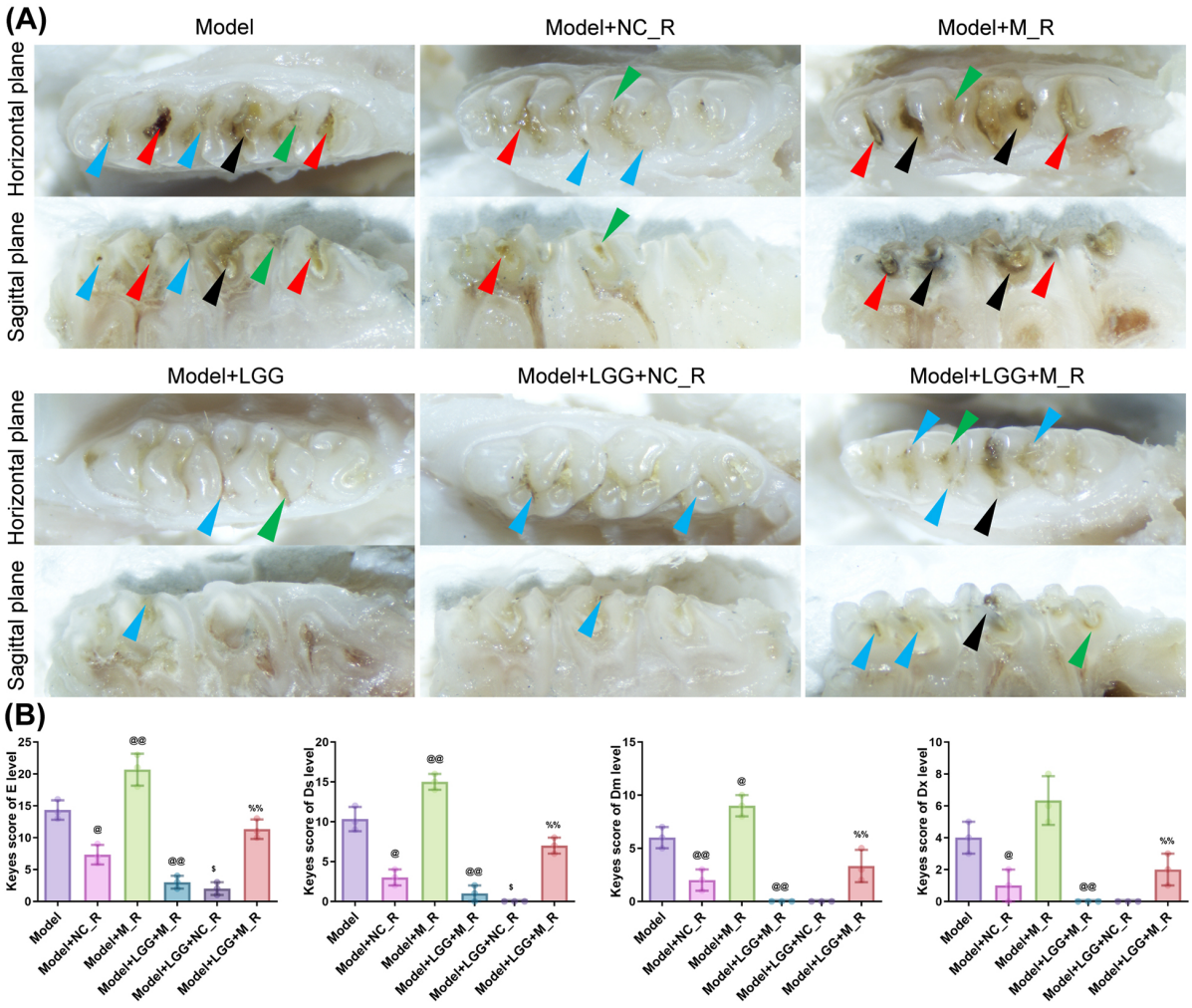

Fig. 5. Effects of different treatments on caries severity in rat molars observed under a stereomicroscope. (A) Stereoscopic microscope was used to observe the horizontal and sagittal sectional views of mandibular molars of rats in each group. Note: the blue arrows indicate E-level caries, the green arrows indicate Ds-level caries, the red arrows indicate Dm-level caries, and the black arrows indicate Dx-level caries. (B) Changes of E, Ds, Dm and Dx caries degree of molars in rats of each group ($n = 3$). Data are presented as mean ± SD. $^{@}p < 0.05$, $^{@@}p < 0.01$ *vs*. Model group; $^{\$}p < 0.05$ *vs*. Model+NC_R group; $^{\%\%}p < 0.01$ *vs*. Model+M_R group.

group, both the Model+NC_R and Model+LGG groups showed significant increases in these three parameters, while the Model+M_R group demonstrated a further significant decrease ($p < 0.05$). In comparison with the Model+NC_R group, the Model+LGG+NC_R group had significantly higher enamel surface area, volume, and mineral density ($p < 0.05$). Relative to the Model+M_R group, the Model+LGG+M_R group showed significantly higher enamel surface area and mineral density ($p < 0.05$).

Effects of Different Treatments on Caries Severity in Rat Molars Observed Under a Stereomicroscope

Caries severity (graded as E, Ds, Dm, and Dx) in rat molars was observed and assessed under a stereomicroscope. Compared with the Model group, both the Model+NC_R and Model+LGG+M_R groups showed significant reductions in caries scores at all levels (E, Ds, Dm, and Dx) (Fig. 5A,B), whereas the Model+M_R group exhibited significant increases in caries severity at the E, Ds, and Dm levels ($p < 0.05$). Compared with the Model+NC_R group, the Model+LGG+NC_R group demonstrated a further significant decrease in caries scores at the E and Ds levels. In contrast to the Model+M_R group, the Model+LGG+M_R group showed significant reductions in caries severity across all levels (E, Ds, Dm, and Dx) ($p < 0.05$).

Discussion

By systematically integrating microbiome and metabolomics technologies, this study revealed the regulatory effects of probiotic interventions on oral microecology and metabolites. The experimental procedure diagram was presented in **Supplementary Fig. 6**. We observed

that the dental plaque microbial community in the caries model group exhibited typical ecological imbalance characteristics: the abundance of cariogenic bacteria such as *Streptococcus mutans* was significantly increased, while health-associated genera such as *Veillonella* were markedly reduced. This finding aligns with previous studies indicating that caries development is accompanied by the overgrowth of specific pathogenic bacteria and a reduction in beneficial bacteria [23,24].

Dental caries is a chronic progressive disease triggered by an imbalance in the oral microbial community, characterized by persistent destruction of tooth hard tissues. This pathological process is closely associated with the formation of dental plaque biofilm, which not only provides structural support for microbial colonization but also significantly enhances their pathogenicity and environmental adaptability. Streptococcus mutans is currently recognized as the primary cariogenic pathogen. By forming highly structured biofilms on tooth surfaces, it not only creates a microecological niche for its own aggregation and proliferation as well as that of other pathogenic bacteria but also significantly elevates its virulence expression and enhances resistance to host immune clearance and antibiotic treatment [25]. In this study, probiotic LGG intervention not only effectively inhibited the overgrowth of *S. mutans* but also promoted the restoration of health-associated genera. This effect was particularly evident in the M_LGG and M_LGG+NC_R groups, suggesting that probiotics may reconstruct oral microecological balance through multiple mechanisms, such as competitive colonization and the secretion of metabolic products. In contrast, the microbial structure of the M_R group more closely resembled that of the Model group, indicating that simply transplanting caries-associated microbiota may not reverse microecological imbalance.

From a metabolic perspective, the Model group showed significant enrichment in carbohydrate metabolism pathways, which is directly related to the pathogenic mechanism whereby cariogenic bacteria continuously produce acid through glycolysis, thereby forming an acidic microenvironment [26]. Conversely, the NC group and probiotic intervention groups exhibited greater activity in pathways such as lipid metabolism and cofactor metabolism, suggesting that a healthy oral environment may depend on a more balanced metabolic network. Notably, the sphingolipid metabolism pathway demonstrated the highest significance in differential metabolite enrichment analysis. Sphingolipids are not only essential components of cell membranes but also participate in processes such as cell signaling, inflammatory regulation, and antimicrobial defense [27]. The activation of this pathway may represent an important host defense mechanism, and probiotic intervention may enhance oral resistance to cariogenic bacteria by regulating this pathway.

This study also systematically identified multiple differential metabolites closely associated with caries development and probiotic intervention. Metabolites significantly upregulated in the Model group, such as Isovaleramide and PC(P-16:0_18:2(9Z,12Z)), may serve as potential biomarkers of the cariogenic process, while downregulated metabolites like (1s,2s,3r,4r)-4-Aminocyclopentane-1,2,3-Triol may play important roles in maintaining oral health. Probiotic intervention, particularly the combined application of LGG and NC_R, significantly reversed the levels of most abnormal metabolites, further confirming the potential of probiotics to exert anti-caries effects through metabolic reprogramming.

Dental plaque is a complex biofilm system attached to tooth enamel surfaces or roots, primarily composed of microbial cells, their secreted extracellular polysaccharides and proteins, and deposited minerals [28]. From a structure-function correlation perspective, the observations from Micro-CT and stereomicroscopy were highly consistent with the aforementioned molecular findings. Probiotic interventions significantly improved enamel surface area, volume, and mineral density while reducing caries severity scores, confirming their protective effects on tooth hard tissues at the macroscopic level. This protective effect likely stems from the dual regulatory effects of probiotics on oral microecology and host metabolism.

This study has several limitations. Although animal models can simulate key features of human caries, species differences still need to be considered. Also, the differential metabolites and pathways currently identified require further functional validation. Additionally, the optimal probiotic combinations, administration timing, and long-term effects warrant deeper exploration. Future research could further integrate metagenomics, metabolic flux analysis, and other technologies to systematically analyze the probiotic interaction network at a multi-omics level and validate its translational potential through clinical studies.

Conclusion

In summary, this study reveals a novel mechanism underlying the anti-caries effect of probiotics from the perspective of microbe-metabolite interactions. Probiotics not only optimize the structure of the oral microbial community but also exert multi-faceted protective effects by regulating the host metabolic network, particularly key pathways such as sphingolipid metabolism. This provides an important theoretical basis for developing precise caries prevention strategies based on microecological regulation.

Availability of Data and Materials

The data presented in this study are available upon request from the corresponding author.

Author Contributions

MS: Conceptualization, Data curation, Formal analysis, Funding acquisition, Investigation, Methodology, Project administration, Resources, Supervision, Validation, Visualization, Writing—original draft, Writing—review & editing. The author gave final approval of the version to be published. The author has participated sufficiently in the work to take public responsibility for appropriate portions of the content and agreed to be accountable for all aspects of the work in ensuring that questions related to its accuracy or integrity.

Ethics Approval and Consent to Participate

The animal ethics in this study complies with The ARRIVE guidelines 2.0. All animal experimental operations in this study were approved by laboratory animal management and ethics committee of Hangzhou Hunter Testing Biotechnology Co., Ltd. (IACUC/HTYJ-11746-93).

Acknowledgment

Not applicable.

Funding

This work was supported by the Shaoxing Health Science and Technology Plan Project [grant number 2023SKY097].

Conflict of Interest

The author declares no conflict of interest.

Supplementary Material

Supplementary material associated with this article can be found, in the online version, at https://doi.org/10.24976/Discov.Med.202638208.118.

References

[1] Folayan MO, Ramos-Gomez F, Sabbah W, El Tantawi M. Editorial: Country profile of the epidemiology and clinical management of early childhood caries, volume II. Frontiers in Public Health. 2023; 11: 1201899. https://doi.org/10.3389/fpubh.2023.1201899.

[2] Maklennan A, Borg-Bartolo R, Wierichs RJ, Esteves-Oliveira M, Campus G. A systematic review and meta-analysis on early-childhood-caries global data. BMC Oral Health. 2024; 24: 835. https://doi.org/10.1186/s12903-024-04605-y.

[3] Li J, Fan W, Zhou Y, Wu L, Liu W, Huang S. The status and associated factors of early childhood caries among 3- to 5-year-old children in Guangdong, Southern China: a provincial cross-sectional survey. BMC Oral Health. 2020; 20: 265. https://doi.org/10.1186/s12903-020-01253-w.

[4] Li F, Wu SC, Zhang ZY, Lo ECM, Gu WJ, Tao DY, *et al*. Trend on dental caries status and its risk indicators in children aged 12 years in China: a multilevel analysis based on the repeated national cross-sectional surveys in 2005 and 2015. BMC Public Health. 2021; 21: 2285. https://doi.org/10.1186/s12889-021-12262-x.

[5] Chen Z, Zhu J, Zhao J, Sun Z, Zhu B, Lu H, *et al*. Dental caries status and its associated factors among schoolchildren aged 6-8 years in Hangzhou, China: a cross-sectional study. BMC Oral Health. 2023; 23: 94. https://doi.org/10.1186/s12903-023-02795-5.

[6] Loesche WJ, Eklund S, Earnest R, Burt B. Longitudinal investigation of bacteriology of human fissure decay: epidemiological studies in molars shortly after eruption. Infection and Immunity. 1984; 46: 765–772. https://doi.org/10.1128/iai.46.3.765-772.1984.

[7] Corby PM, Lyons-Weiler J, Bretz WA, Hart TC, Aas JA, Boumenna T, *et al*. Microbial risk indicators of early childhood caries. Journal of Clinical Microbiology. 2005; 43: 5753–5759. https://doi.org/10.1128/JCM.43.11.5753-5759.2005.

[8] Tanner ACR, Mathney JMJ, Kent RL, Chalmers NI, Hughes CV, Loo CY, *et al*. Cultivable anaerobic microbiota of severe early childhood caries. Journal of Clinical Microbiology. 2011; 49: 1464–1474. https://doi.org/10.1128/JCM.02427-10.

[9] Qudeimat MA, Alyahya A, Karched M, Behbehani J, Salako NO. Dental plaque microbiota profiles of children with caries-free and caries-active dentition. Journal of Dentistry. 2021; 104: 103539. https://doi.org/10.1016/j.jdent.2020.103539.

[10] Boisen G, Brogårdh-Roth S, Neilands J, Mira A, Carda-Diéguez M, Davies JR. Oral biofilm composition and phenotype in caries-active and caries-free children. Frontiers in Oral Health. 2024; 5: 1475361. https://doi.org/10.3389/froh.2024.1475361.

[11] Liang J, Liang D, Liang Y, He J, Zuo S, Zhao W. Effects of a derivative of reutericin 6 and gassericin A on the biofilm of Streptococcus mutans in vitro and caries prevention in vivo. Odontology. 2021; 109: 53–66. https://doi.org/10.1007/s10266-020-00529-5.

[12] Luo SC, Wei SM, Luo XT, Yang QQ, Wong KH, Cheung PCK, *et al*. How probiotics, prebiotics, synbiotics, and postbiotics prevent dental caries: an oral microbiota perspective. NPJ Biofilms and Microbiomes. 2024; 10: 14. https://doi.org/10.1038/s41522-024-00488-7.

[13] Krupa NC, Thippeswamy HM, Chandrashekar BR. Antimicrobial efficacy of Xylitol, Probiotic and Chlorhexidine mouth rinses among children and elderly population at high risk for dental caries - A Randomized Controlled Trial. Journal of Preventive Medicine and Hygiene. 2022; 63: E282–E287. https://doi.org/10.15167/2421-4248/jpmh2022.63.2.1772.

[14] Homayouni Rad A, Pourjafar H, Mirzakhani E. A comprehensive review of the application of probiotics and postbiotics in oral health. Frontiers in Cellular and Infection Microbiology. 2023; 13: 1120995. https://doi.org/10.3389/fcimb.2023.1120995.

[15] Nizami MZI, Chu S, Chu S, Chu CH. Probiotics for caries prevention: A narrative review. Journal of Applied Biomaterials & Functional Materials. 2025; 23: 22808000251376427. https://doi.org/10.1177/22808000251376427.

[16] Chen Y, Hao Y, Chen J, Han Q, Wang Z, Peng X, *et al*. Lactiseibacillus rhamnosus inhibits the development of dental caries in rat caries model and in vitro. Journal of Dentistry. 2024; 149: 105278. https://doi.org/10.1016/j.jdent.2024.105278.

[17] Nie Q, Wan X, Tao H, Yang Q, Zhao X, Liu H, *et al*. Multifunction screening of probiotics to improve oral health and evaluating their efficacy in a rat periodontitis model. Frontiers in Cellular and Infection Microbiology. 2023; 13: 1261189. https://doi.org/10.3389/fcimb.2023.1261189.

[18] Zhang J, Wang Q, Duan Z. Preventive effects of probiotics on dental caries in vitro and in vivo. BMC Oral Health. 2024; 24: 915. https://doi.org/10.1186/s12903-024-04703-x.

[19] Nivetha S, Murugan M, Durgadevi C. Restraint of dental caries-inducing Streptococcus mutans MTCC497 by potential oral bacterial metabolite - In vitro and In vivo analysis in Caenorhabditis elegans. Microbial Pathogenesis. 2025; 206: 107810. https://doi.org/10.1016/j.micpath.2025.107810.

[20] Zheng ZY, Chen CL, Chen ZG, Zhang QW, Fan QL, Chen S. Screening of probiotics for preventing dental caries and evaluating the effectiveness in improving dental caries in rats. Food and Fermentation Industries. 2025; 51: 82–88. (In Chinese)

[21] Liu R, Liu Y, Yi J, Fang Y, Guo Q, Cheng L, *et al*. Imbalance of oral microbiome homeostasis: the relationship between microbiota and the occurrence of dental caries. BMC Microbiology. 2025; 25: 46. https://doi.org/10.1186/s12866-025-03762-6.

[22] Keyes PH. Dental caries in the molar teeth of rats. II. A method for diagnosing and scoring several types of lesions simultaneously. Journal of Dental Research. 1958; 37: 1088–1099. https://doi.org/10.1177/00220345580370060901.

[23] Dinis M, Traynor W, Agnello M, Sim MS, He X, Shi W, *et al*. Tooth-Specific *Streptococcus mutans* Distribution and Associated Microbiome. Microorganisms. 2022; 10: 1129. https://doi.org/10.3390/microorganisms10061129.

[24] Wang Y, Zhang J, Chen X, Jiang W, Wang S, Xu L, *et al*. Profiling of Oral Microbiota in Early Childhood Caries Using Single-Molecule Real-Time Sequencing. Frontiers in Microbiology. 2017; 8: 2244. https://doi.org/10.3389/fmicb.2017.02244.

[25] Yoon S, Park S, Jung SE, Lee C, Kim WK, Choi ID, *et al*. Fermented Milk Containing *Lacticaseibacillus rhamnosus* SNU50430 Modulates Immune Responses and Gut Microbiota in Antibiotic-Treated Mice. Journal of Microbiology and Biotechnology. 2024; 34: 1299–1306. https://doi.org/10.4014/jmb.2401.01012.

[26] Kameda M, Abiko Y, Washio J, Tanner ACR, Kressirer CA, Mizoguchi I, *et al*. Sugar Metabolism of *Scardovia wiggsiae*, a Novel Caries-Associated Bacterium. Frontiers in Microbiology. 2020; 11: 479. https://doi.org/10.3389/fmicb.2020.00479.

[27] Albi E, Alessenko A, Grösch S. Sphingolipids in Inflammation. Mediators of Inflammation. 2018; 2018: 7464702. https://doi.org/10.1155/2018/7464702.

[28] Jakubovics NS, Goodman SD, Mashburn-Warren L, Stafford GP, Cieplik F. The dental plaque biofilm matrix. Periodontology 2000. 2021; 86: 32–56. https://doi.org/10.1111/prd.12361.